Available online at www.sciencedirect.com

ScienceDirect

journal homepage: www.elsevier.com/locate/he

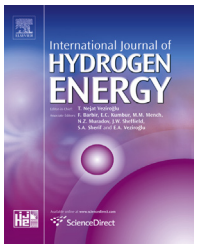

Cathode materials for ceramic based microbial fuel cells (MFCs)

Carlo Santoro [a], Kateryna Artyushkova [a], Iwona Gajda [b], Sofia Babanova [a], Alexey Serov [a], Plamen Atanassov [a], John Greenman [c], Alessandra Colombo [d], Stefano Trasatti [d], Ioannis Ieropoulos [b,c], Pierangela Cristiani [e,*]

[a] Center for Micro-Engineered Materials (CMEM), Department of Chemical and Biological Engineering, University of New Mexico, Albuquerque, NM, USA

[b] Bristol BioEnergy Centre, Bristol Robotics Laboratory, T-Block, UWE, Bristol, Coldharbour Lane, Bristol BS16 1QY, UK

[c] Biological, Biomedical and Analytical Sciences, University of the West of England, BS16 1QY, Bristol, UK

[d] Università degli Studi di Milano, Department of Chemistry, Via Golgi 19, 20133 Milan, Italy

[e] RSE – Ricerca sul Sistema Energetico S.p.A., Sustainable Development and Energy Sources Department, Via Rubattino 54, 20134 Milan, Italy

ARTICLE INFO

Article history:
Received 15 March 2015
Received in revised form
30 June 2015
Accepted 10 July 2015
Available online 30 July 2015

Keywords:
Carbonaceous materials
Ceramic separator
Current production
Morphology
Fe-AAPyr catalyst

ABSTRACT

This study showed the electrochemical performance of different cathode electrodes tested on a ceramic separator functioning as a cation exchange membrane. Particularly, three different carbonaceous-based materials (carbon cloth (CC), carbon mesh (CM) and carbon veil (CV)) have been used as an electrode and as the current collector. When used as an electrode, CC outperformed the others. The carbonaceous materials have been modified using conductive paint (PA) and micro porous layer (MPL). With these modifications, the current output was two–three times higher. Generally, the current produced was slightly higher with MPL treatment compared to PA except in the case of CV-MPL that had lower output probably due to the negative effect of the heat treatment on the mechanical strength of the CV. In the case of PA, the current collectors do not seem to affect the output. The same consideration can also be done for the MPL except for the CV. The surface morphology seems to explain the results. Linear correlation was found between current produced and nanoscale roughness and skewness. The results indicated that those morphological parameters increased the contact between the cathode and the ceramic surface, thus enhancing the current generated. The further addition of the inorganic non-platinum group catalyst (Fe-AAPyr) on the surface significantly enhanced the performances. Following MPL modification and MPL-Fe-AAPyr addition, CM was the most cost effective support. CV was the most cost effective support with PA modification.

Copyright © 2015, Hydrogen Energy Publications, LLC. Published by Elsevier Ltd. All rights reserved.

* *Corresponding author*. RSE – Ricerca sul Sistema Energetico S.p.A., Sustainable Development and Energy Sources Department, 20133 Milan, Italy. Tel.: +39 0239924655; fax: +39 0239924608.
E-mail address: pierangela.cristiani@rse-web.it (P. Cristiani).

http://dx.doi.org/10.1016/j.ijhydene.2015.07.054

0360-3199/Copyright © 2015, Hydrogen Energy Publications, LLC. Published by Elsevier Ltd. All rights reserved.

Introduction

Water availability has been an important global challenge and consequently, water treatment is critical in successfully addressing this problem. The common technologies available for wastewater treatment are very efficient in degrading organics, but very expensive to operate, mainly due to the electricity necessary for mixing and pumping oxygen. Alternative approaches, such as Microbial Fuel Cells (MFCs), have been explored to make the process more efficient and to decrease significantly the cost [1,2]. This emerging bioelectrochemical technology is not only able to degrade organics but also to transform the chemical energy stored in compounds such as water pollutants into useful electricity [1,2]. The electricity generated can be used for small-scale real applications [3–5]. However, this technology is still at the lab scale of development.

Major concerns related to MFC utilization are: i) the relative high cost of the electrode materials [6,7]; ii) the low power output caused by the unoptimized anodic [8] and cathodic [9] conversion processes.

Anodic processes are mainly controlled by the electrically active bacteria, which upon adhering to the electrode, can degrade organics releasing and transferring electrons to the conductive electrode. Electrons moving through the external circuit generate electricity that can be harvested and successfully utilized [3–5]. The understanding of bacteria attachment [10], electron transfer [11], biofilm formation and development [12,13] bacteria selection [14] is still a matter of ongoing investigation.

Cathode processes are mainly affected by the high overpotential caused by the low electrochemical activity of the catalysts used (inorganic or biotic) at neutral pH [15]. Although it has been shown [16,17] that specific enzymes can significantly lower the overpotential of oxygen reduction reaction (ORR) at neutral pH, utilization of carbonaceous [6,18] or transition metal-based [19,20] catalysts is preferred due to the higher availability, low cost and durability. Platinum has been traditionally used as a cathodic catalyst in MFCs [21] but it has been shown to suffer from rapid decrease in performance due to the fast poisoning effect of sulfide presence in the wastewater [22]. Two different avenues are currently being exploited aiming at a finding the trade-off between cost and efficiency of ORR: i) catalysts based on utilization of carbon-based materials, having high conductivity and high surface area [6]; ii) inorganic catalysts such as iron (Fe) [23], cobalt (Co) [24,25] and manganese (Mn) [26].

Moreover, the current collector design is also very important for guaranteeing high cathode performances. Several current collectors have been used in MFCs mainly based on carbonaceous materials and particularly carbon veil [27,28], carbon cloth [29], carbon paper [30] and carbon felt [30]. Also, metallic meshes have been used, based on corrosion proof stainless steel [31]. An understanding of the best performing and cost-effective material is still necessary.

Some studies have shown that the formation of biofilm due to the direct exposure of the anodic solution in membraneless MFC configuration lead to an enhancement in the cathode performance as a result of a biocathode formation [32,33]. The OH^- production during the ORR leads to cathode alkalization [34,35] and calcium and sodium carbonate precipitation on the cathode [36], lowering its long-term operation [32]. Consequently, the option of using a solid separator able to decrease the negative effects of cathode alkalization seems to be reasonable for preventing cathode deactivation and keeping the anode chamber under strictly anaerobic conditions. Anionic and cationic exchange membranes have been used previously in a single chamber or double chamber MFCs [37]. It has been shown that cationic membranes are preferable than the anionic membranes most likely because they prevent an accumulation of protons at the anode that inhibits bacterial metabolism [38]. The main problem related with solid polymeric separators is the high cost of the membrane that makes them not suitable for a large-scale operation [39]. Recently, MFCs with ceramic cation exchange membranes, utilized as a physical separator between the anode and cathode have been successfully developed and explored [39,40]. The main advantages of ceramic separators are: i) low cost; ii) high ions selectivity; iii) high mechanical strength and iv) high durability [39,40].

This work focuses on the electrochemical analysis of different low-cost carbonaceous materials suitable for the design of cathodes in ceramic MFCs. Carbonaceous materials (veil, cloth and mesh) have been tested: i) without any pretreatment, ii) coated with a micro porous layer (MPL); iii) coated with a conductive carbon paint. The performance of low-cost non-platinum group metals (non-PGM) Fe-Aminoantipyrine (Fe-AAPyr) has also been studied, demonstrating promising results compared to other materials. Cost-performance analysis of the different options has been also carried out, in the light of future large-scale applications.

Materials and method

Cathode materials

Different materials have been tested as cathodes or cathodic support in ceramic-based MFC. Particularly, three carbonaceous electron collectors have been used identified as carbon veil (CV), carbon cloth (CC) and carbon mesh (CM) (Fig. 1). Those materials were purchased from PRF Composite Materials (Dorset, UK), Saati (Legnano, Italy) and Electromar (Milan, Italy), respectively. CV, CC, and CM have been used as controls during the experiments.

Modifications were done with the addition of conductive paint from TIMCAL Ltd. Switzerland (PA) or a micro porous layer (MPL). The materials with PA and MPL have been additionally modified with Fe-AAPyr as a catalyst for ORR. PA was applied on the carbonaceous support using a brush, covering the entire surface with a PA loading of 40 ± 10 mg cm^{-2}. MPL was done similarly as previously described [41]. In summary, 0.7 g of TIMCAL carbon powder was put in a beaker with 9.1 mL of distilled water and 21.5 mL of nonionic surfactant (Triton X100, Sigma Aldrich) and then mixed for 10 min using a spatula. Then, 1 g of PTFE (Sigma Aldrich) was added, and the slurry has been mixed for another 10 min. At last, 2.75 g of carbon powder was added, and the overall content was mixed for an additional 10 min. The resultant mixture was then

applied on the CV, CC and CM using a brush. Thermal treatment has followed, where the materials coated with the MPL were inserted in an oven and heated up at 250 °C for almost 2 h and cool down at room temperature before utilization. The MPL loading was 50 ± 10 mg cm^{-2}.

Fe-AAPyr has been prepared as previously reported [23] and added on the MPL surface using a micropipette covering the entire surface. Particularly, Fe-AAPyr has been mixed with Nafion and isopropanol and put into an ultrasonic bath for 15 min. Fe-AAPyr loading on the cathode surface was 0.3 mg cm^{-2}.

Surface morphology analysis

Scanning Electron Microscopy (SEM) images have been taken using a SEM TESCAN mod. Mira II. Three images for each sample (CV, CV-PA, CV-MPL, CC, CC-PA, CC-MPL, CM, CM-PA, CM-MPL) at two different magnifications (100× and 10000×) were acquired. The morphological features of the surfaces were obtained using previously reported image processing tools in Matlab [42]. A high-pass filter was applied to remove the low-frequency component, and a low-pass filter to remove the high-frequency component from the images to produce roughness and waviness image components, respectively [43]. At 100× magnification, the high-frequency component images correspond to roughness in the range of 10–33 μm, and the low-frequency component images correspond to 100–400 μm. At 10000× magnification, filtering separates the images into the low-frequency component at 1.3–5.5 μm scale and a high-frequency component at 60–500 nm. From all these waviness and roughness images, we have extracted roughness (Ra) and skewness (Rsk), which point to the domination of pores or peaks in the image.

Chemical surface analysis

Samples were characterized using a Kratos AXIS DLD Ultra X-ray photoelectron spectrometer with monochromatic Al Kα source operating at 225 W. No charge compensation was necessary. Survey spectra were acquired at pass energy (PE) of 80 eV, and C 1s and O 1s high-resolution spectra were acquired at PE of 20 eV. Data analysis and quantification were performed using the CASAXPS software. A linear background was used for C 1s and O 1s spectra. Quantification utilized sensitivity factors provided by the manufacturer. A 70% Gaussian/30% Lorentzian line shape was used for the curve-fits.

Ceramic cell set-up

Ceramic cylinders were made from porous earthenware material (International Biological Laboratories, Haryana, India). It was used as a physical separator or a membrane between the internal volume and the external face. In a typical MFC configuration, the anode could be inserted in the internal volume with the cathode on the external face or vice versa the anode on the external face with the cathode inserted internally. In the present study, the experimental setup involved cathode materials with a geometric area of 108 cm^2 being wrapped around the cylindrical ceramic tube (Fig. 2a). The average dimensions of the ceramic were: external diameter of 4.24 cm, the height of 8.135 cm, wall thickness of 3.45 mm and an internal volume of 80.5 mL.

Inside the cylindrical ceramic, phosphate buffer saline (PBS, 50 mM) with 50 mM KCl was used as an electrolyte (Fig. 2b). The pH of the solution was 7.3–7.4 simulating the typical conditions of a wastewater.

Electrochemical analysis

Linear Sweep Voltammetry (LSV) using a three-electrode configuration was used for materials characterization, with platinum mesh as the counter, saturated calomel (SCE, + 0.241 V vs SHE) as the reference and the actual cathode as the working electrode, as shown in Fig. 2 b. The working cell has been left at open circuit potential (OCP) for at least 1 h and then the LSV was performed. The scan rate used was 0.2 mV s^{-1} as previously reported [41].

Cost-analysis

The cost-analysis was done considering the price of the support materials. Particularly, the cost was 28.5 US$ m^{-2} for CC, 16.3 US$ m^{-2} for the CM and 15.4 US$ m^{-2} for CV. Being the area of a single cathode 108 cm^2, the cost for each cathode was 0.308 US$, 0.176 US$ and 0.166 US$ for CC, CM, and CV, respectively.

The cost of the conductive painting (PA) such as that of the carbon particle (MPL) was not disclosed by the supplier, but it is considered to be negligible compared to the cost of the cathode materials, as the carbon powder industrial cost is in the order of magnitude of 1 $ per 10 kg. The cost of the cathode with the addition of PA or MPL will increase, especially for the process with MPL, which includes heating treatment and the addition of PTFE. Since the quantity of PA or MPL applied on the support was the same, the costs due to the process of cathode preparation should be similar to that of the other low temperature fuel cells already industrialized, and the difference is expected to be mainly due to the support cost that has been previously identified.

A rough estimation of the catalyst Fe-AAPyr cost considering the materials price showed by Sigma Aldrich catalog was previously done at 3.5 US$ g^{-1} [23]. Due to the catalyst loading of 0.3 mg cm^{-2}, the additional cost due to the catalyst addition was 0.11 US$.

Results

Chemical analysis

Table 1 shows elemental composition and carbon chemical speciation of support materials as obtained from high resolution XPS analysis. Elemental composition of support materials is similar with approximately 11–19 at.% of oxygen present, with CC having the lowest and CM the highest amount. The presence of nitrogen and sodium (2–3 at.%) was detected in CC and CB supports. Chemical properties of carbon were evaluated from chemical speciation obtained from high-resolution C 1s spectra shown in Fig. 3. CM has lowest graphitic content (peak at 284.6 eV and shake-up at 290.9 eV)

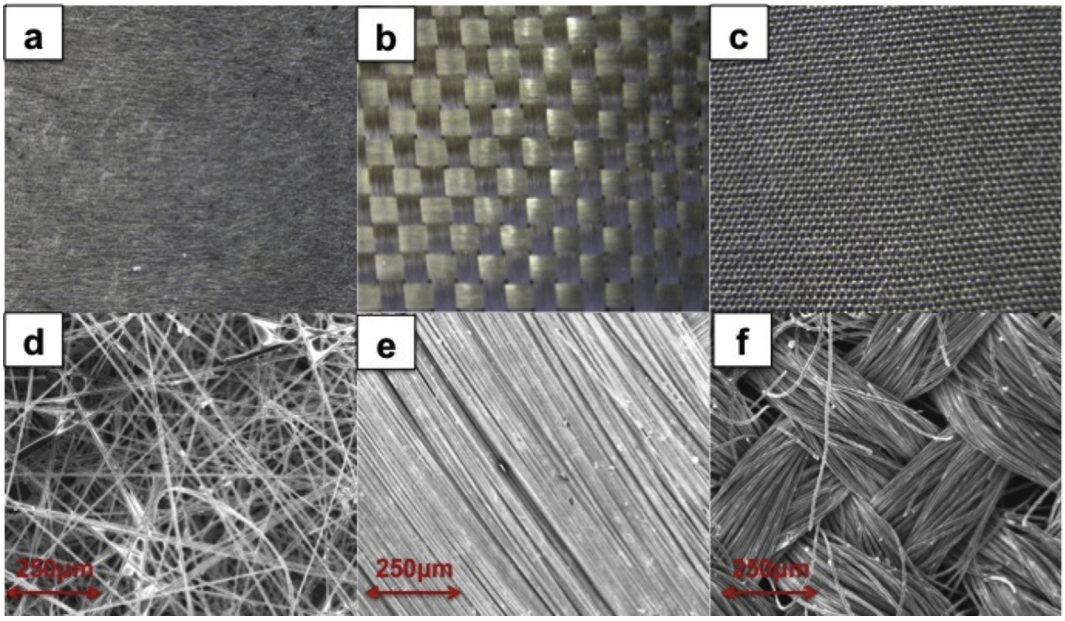

Fig. 1 – Camera Photo of CV (a), CM (b), CC (c) and SEM images (1.2 mm × 1.2 mm) of CV (d), CM (e), CC (f).

and the highest amount of different types of C–O groups, i.e. C–O at 286.4 eV, C=O at 287.5 eV and COOH at 292.2 eV. These three peaks were summed up to represent the total amount of surface oxides present in Table 1 – %CxOy. The peak due to secondary shifted carbons, such as C^{*}-C_x-O_y, confirms high oxygen functionalization for CM support. The CC has the highest graphitic content, and a small amount of surface oxides detected. The CV is similar to CC with slightly higher amounts of surface oxides present.

Morphological analysis

The SEM images processing led to important conclusions regarding the surface roughness and porosity of the materials tested. It can be noticed that CV and CC have similar roughness at the micro scale (100–400 μm) that is slightly higher than the roughness of CM (Fig. 4a). On the contrary, CC and CM have higher roughness at the nano scale (60–500 nm) compared to CV (Fig. 4b), with CC having the highest roughness at both scales. CM has larger fibers compared to CV that in a higher resolution image appear much smoother in comparison to CV, but at nano scale they showed higher unevenness that is overlooked without the filtering and DIP procedure we have applied (Fig. 4b). Generally, independently of the support adopted, the addition of PA and MPL led to an increase in the roughness in the nano scale 60–500 nm (Fig. 4b) and decrease of the roughness at the micro scale 100–400 μm (Fig. 4a). These results can be explained by the coating and/or the PA and MPL are filling the gaps between the carbon fibers making the surface more uniform at the micro-scale (Fig. 4a), while increasing the roughness at smaller nano-scale due to the intrinsic roughness of the coating itself and/or irregular particles distributed on the substrate. Also the skewness, a metrics of porosity, was calculated for all scales while only the porosity at the nanoscale of 60–500 nm showed important information. In addition, to the increase in nano-roughness as discussed above, the application of coating led to a substantial increase in the porosity at the nano scale (Fig. 4c). The increase in small pores with the addition of coating on top of the support

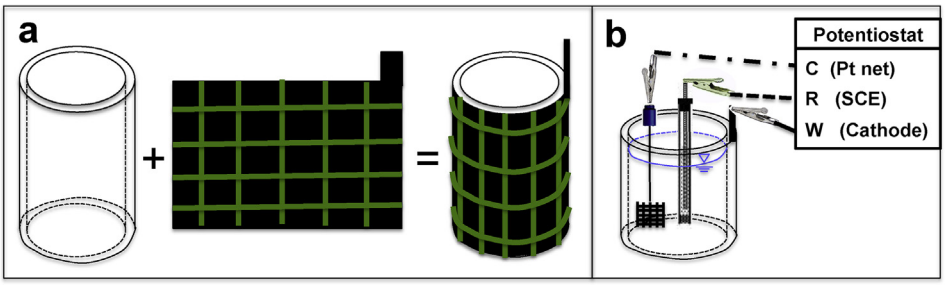

Fig. 2 – Schematic view of the ceramic support with the electrode in contact with the external face (a). Experimental design for the electrochemical measurements in a three-electrode configuration (b).

is causing an increase in nano-roughness that is important characteristics in the fuel cell design as will be discussed below.

Electrochemical results

Single electrode linear sweep voltammetry was done on each material (Fig. 5). The results showed two main important aspects: i) the addition of PA and MPL increased the cathodes performance compared to the raw materials despite similar open circuit potential (OCP); ii) the addition of Fe-AAPyr boosted up both OCP and current generated. More specifically, in the case of CV, the current produced at −0.2 V for CV only was 0.69 ± 0.11 mA and increased 3.6 times with the addition of PA (2.45 ± 0.28 mA) and 2.6 times with the MPL coating (1.78 ± 0.22 mA) (Fig. 5c). When CM was used as current collector, the current produced at −0.2 V was 0.89 ± 0.21 mA for CM only and increased 3 times with the addition of PA (2.68 ± 0.23 mA) and 3.7 times with the MPL coating (3.29 ± 0.29 mA) (Fig. 5b). CC produced a current of 1.07 ± 0.15 mA that increased 2.5 times (2.62 ± 0.15 mA) and 3.1 times (3.34 ± 0.32 mA) due to PA and MPL addition, respectively (Fig. 5a).

A further significant increase in the cathodes performance was obtained with the utilization of Fe-AAPyr catalyst. This catalyst has been used previously in hydrogen PEM fuel cell [44] and double chamber MFC [23] and now for the first time has been characterized by half-cell configuration, simulating a single chamber MFC with ceramic membrane separator. It has been shown previously that Fe-based catalysts possess high electrochemical activity at very acidic or basic pH levels [44]. Despite the utilization of a well-buffered solution (50 mM PBS) with 0.1 M KCl as electrolyte, it has been shown also that severe basic conditions (pH up to almost 14) takes place on the catalytic sites [34,35] that have also been seen previously utilizing wastewater and sodium acetate [45]. The Fe-AAPyr cathodes demonstrated almost doubled current production at −200 mV vs. SCE independently of the support used.

It has to be noted that at pH equal to 7, the theoretical OCP is ~820 mV vs SHE (~570 mV vs SCE) and in this particular study, Fe-AAPyr cathodes showed the highest OCP that was ~205 ± 5 mV vs. SCE (Fig. 5). Lower OCP was recorded when the materials without Fe-AAPyr were investigated. Those values were in the range between 50 and 100 mV vs SCE (Fig. 5). The results underlined a massive overpotential of approximately 360 mV when Fe-AAPyr is utilized and approximately 470–520 mV without it. The high overpotentials are in line with the literature [19] and seem to be the main problem of the cathodes working at neutral pH.

Table 1 – Elemental composition and carbon chemical speciation of supports.

	C 1s %	O 1s %	C=C	C*	%CxOy
CM	81.2	18.8	28.4	22.8	48.8
CC	88.3	11.7	62.6	12.3	25.1
CV	87.2	12.8	49.1	16.6	34.2

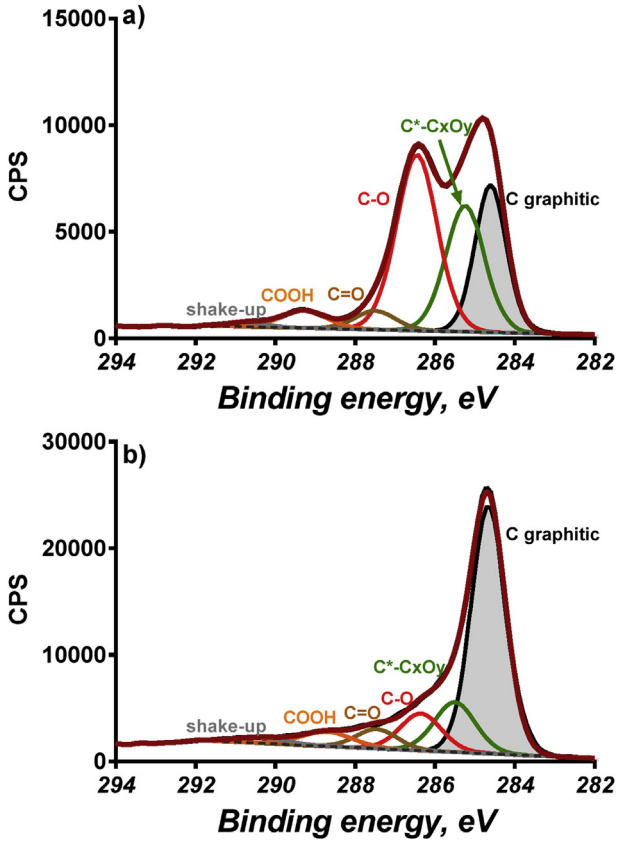

Fig. 3 – High resolution C 1s spectrum for a) CM and b) CC carbon supports.

General trend and cost considerations

To have a complete overview of the results, all the polarization curves for the materials investigated have been overlayed (Fig. 6). Significant difference in the electrochemical performance between the carbonaceous raw materials CV, CC, CM and the same materials after treatment can be noticed. For the raw materials, a comparable electrochemical behavior is observed untill −0.2 V. Between −0.2 V and −0.4 V, CC performed better than CM and the latter outperformed the CV. At potential tested of −0.4 V, the CC produced 1.07 ± 0.15 mA that was 20% higher than CM (0.88 ± 0.21 mA) and 54% CV (0.69 ± 0.11 mA).

These results may be explained by the differences in surface morphology of the carbonaceous supports, especially the roughness and porosity at the nano scale, which correlates linearly with the current produced by the supports themselves (Fig. 7a). CV had the lower current produced and the lower roughness at the nanoscale. The latter may lead to a lower contact between the cathode and the ceramic support and consequently lower performance (Fig. 7). In contrast, both CC and CM are rougher than CV at the nanoscale and the much better contact increased the current generated (Fig. 6). In addition, CC has the highest amount of graphitic carbon detected (Section 3.1) which may improve the overall conductivity of the catalyst. It is important to note, that CV also has higher graphitic content than CM does, but it shows worse performance which is mainly explained by the smallest

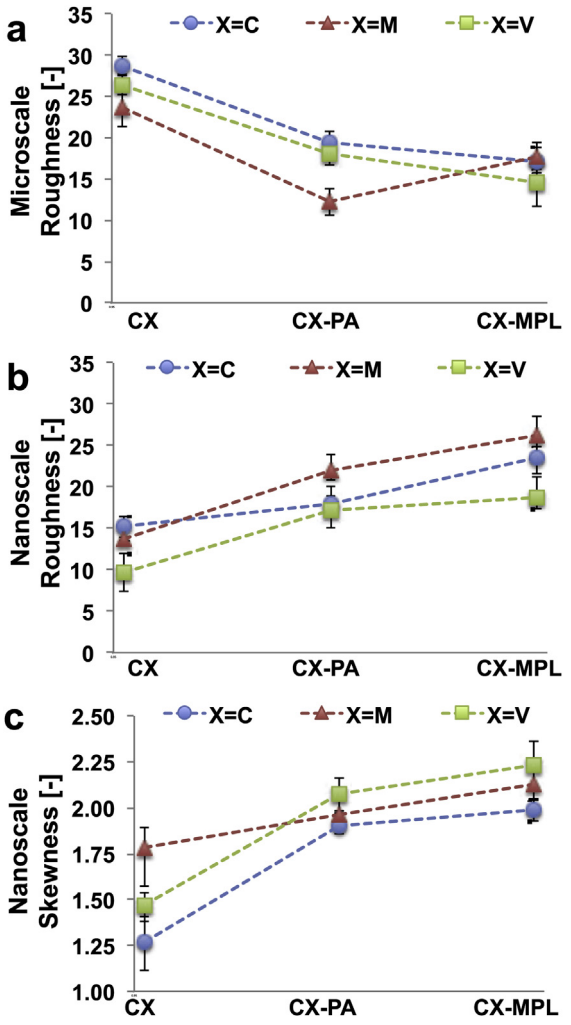

Fig. 4 – Roughness at the micro scale between 100 and 400 μm (a), at the nano scale between 60 and 500 nm (b) and porosity at nanoscale between 60 and 500 nm (c).

nanoroughness of the CV support. CM has the highest amount of carbon surface oxides, as reported by XPS, which results in the material with higher hydrophilic character potentially facilitating dispersion of the FeAAPyr catalysts on the support with MPL added. Combination of chemistry and morphology (nano-porosity and nano-roughness), thus, is responsible for the performance of catalysts supported on the porous carbonaceous supports.

All three carbonaceous materials have been modified by adding PA and MPL, and this modification has increased the performance significantly (Fig. 6). This, at least, doubling of the current output can be due to the fact that the addition of PA or MPL, first of all, increases the conductivity of the material by filling the gaps between the fibers, and, second, dramatically increases the materials roughness at nanoscale (60–500 nm) (Fig. 4b) that is beneficial for a better contact of the cathode with the ceramic membrane. The current produced from all materials investigated (except with Fe-AAPyr) was plotted as a function of the roughness and skewness at nanoscale and a linear dependence with $R^2 > 0.8$ was found (Fig. 7 b and c) indicating that both nanoscale morphological parameters are central to increasing the current output.

Moreover, it can be noticed that the addition of MPL on the surface of the CC and CM is increasing the current output more than the addition of PA (Fig. 6). The opposite result was obtained when CV was used, and this can be due to the thermal treatment that the materials were subjected to after the application of the MPL slurry. In fact, CC and CM have a much higher thickness and mechanical strength compared to CV and, evidently, they better withstand temperatures above 200 °C. A single layer of CV seems not to have enough mechanical strength to support stress for long-term operation but this problem could be solved by utilizing several layers packed one on each other or reinforcing the fibers with addition of low amount of PTFE.

Cost – morphology – performance correlation analysis

The material cost is another fundamental factor to consider for large-scale practical applications. In fact, despite CC performed 20% and 54% higher than CM and CV respectively, CC had the highest cost, which was 43% and 46% higher than CM and CV, respectively. This indicates that CM is the most cost-effective material studied with the lowest cost to produce 1 mA, precisely 0.198 US$ mA^{-1}, followed by the CV (0.24 US$ mA^{-1}) and CC (0.287 US$ mA^{-1}). The cost was calculated considering the current produced at −0.2 V vs. SCE.

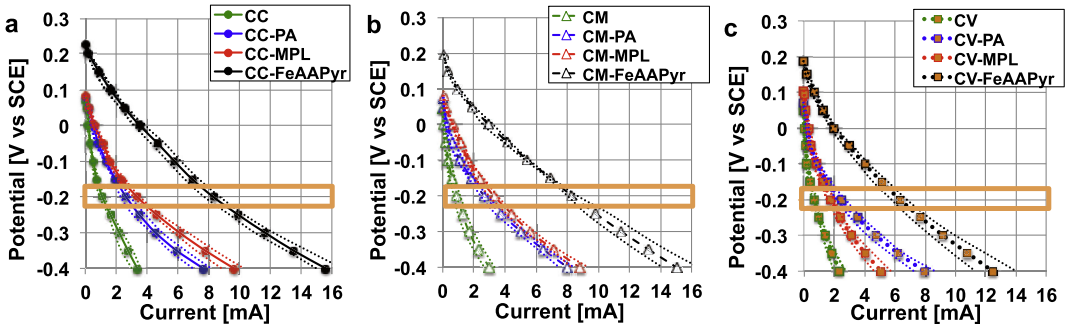

Fig. 5 – Cathode polarization curves of the CC-based cathode (a), a CM-based cathode (b) and CV-based cathode (c). The green line indicates the performances of the support only; the blue line indicates the modification with PA, red line the addition of MPL and the black line the addition of MPL and Fe-AAPyr. (For interpretation of the references to color in this figure legend, the reader is referred to the web version of this article.).

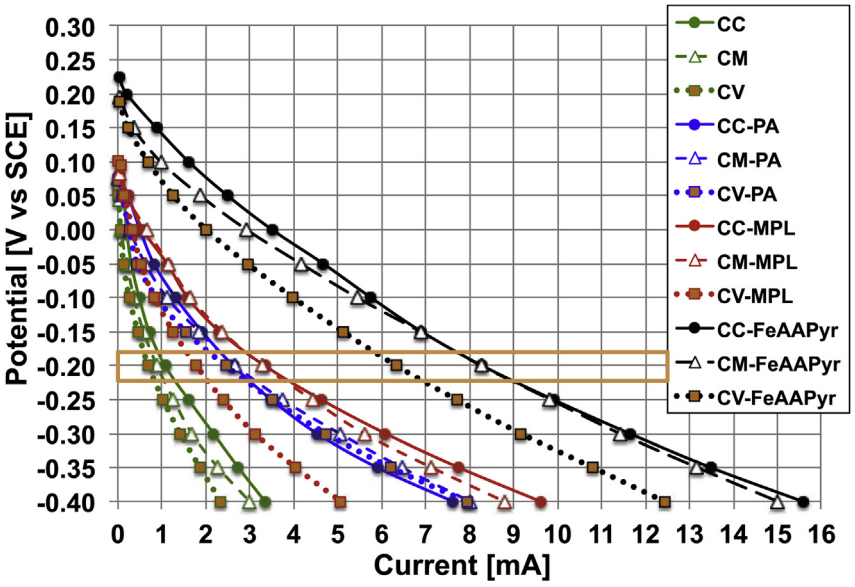

Fig. 6 – Overall electrochemical cathode performances trends.

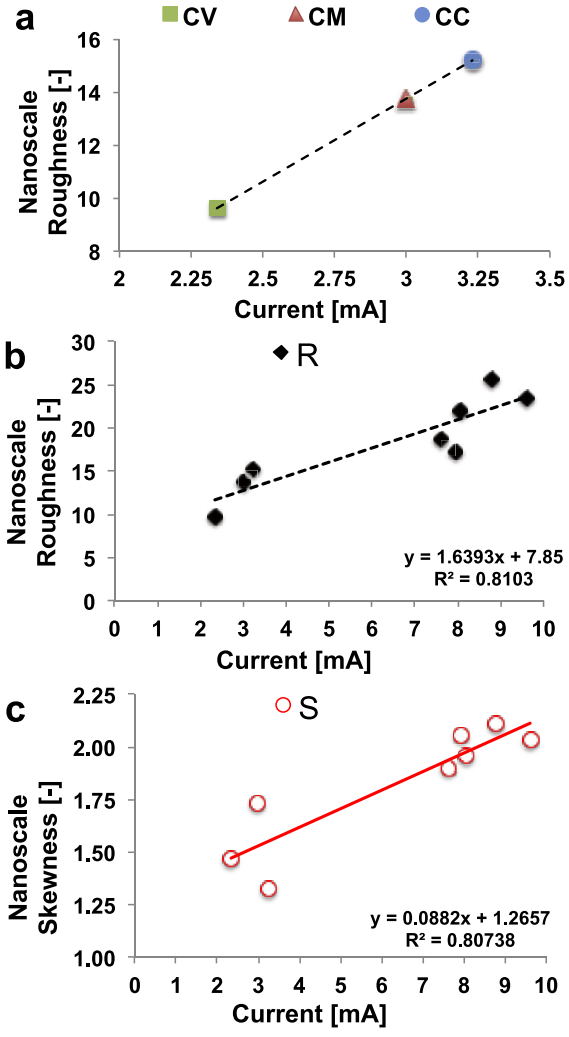

Fig. 7 – Correlation between current produced by the support and the roughness of the support at the nanoscale (60–500 nm) (a). Nanoscale roughness (b) and skewness (c) of the cathodes tested as a function of the current produced.

The addition of PA resulted in similar output independently from the carbonaceous support (CV, CC, CM) (Fig. 6). Consequently, the carbon support with the lowest cost, i.e. CV is the most cost-effective material when PA is utilized. Similar conclusions can be drawn when MPL is added, except the CV-MPL (Fig. 6). Therefore, CM is also the most cost-effective material when MPL is utilized.

The performance was significantly enhanced when non-PGM Fe-AApyr electrocatalyst was utilized (Fig. 8). Similarly, in this case, the support materials did not play an important role in the current generated (Fig. 6). CM was, again, the most cost-effective support to be utilized.

For understanding the effects the morphological properties of the support and the MPL on the performance of Fe-AAPyr based cathodes, principal component analysis was applied to the data table combining the following variables: nano-roughness Ra of the support and MPL, microroughness Ra of the support and MPL, nanoporosity (Rsk) of the support and MPL, cost of the cathodes, current as produced by the system combining Fe-AAPyr, MPL, PA and support and cost/current ratio. Fig. 8 shows that the current generated is dependent on both nano- and micro-roughness of MPL. If the support has initially high nano-roughness it is enhanced even more by the addition of MPL. In terms of performance of the Fe-AAPyr based cathodes, both CM and CC showed similarly good performance, but CC is much more expensive resulting in a high cost/current ratio, making CM the optimal support. CM in combination with MPL results in a morphology with the highest nano and microroughness providing good contact and, therefore, good current collection efficiency.

These results bring to the conclusion that generally, among the materials studied, the support or current collector is not the key factor for the current output, and it is actually the support modification that lead to efficient current densities. Consequently, a lower cost of the support is necessary. In several cases, CC outperformed CM and CV, but due to its high cost, it does not seem suitable for large-scale applications where cost is as important as the performance.

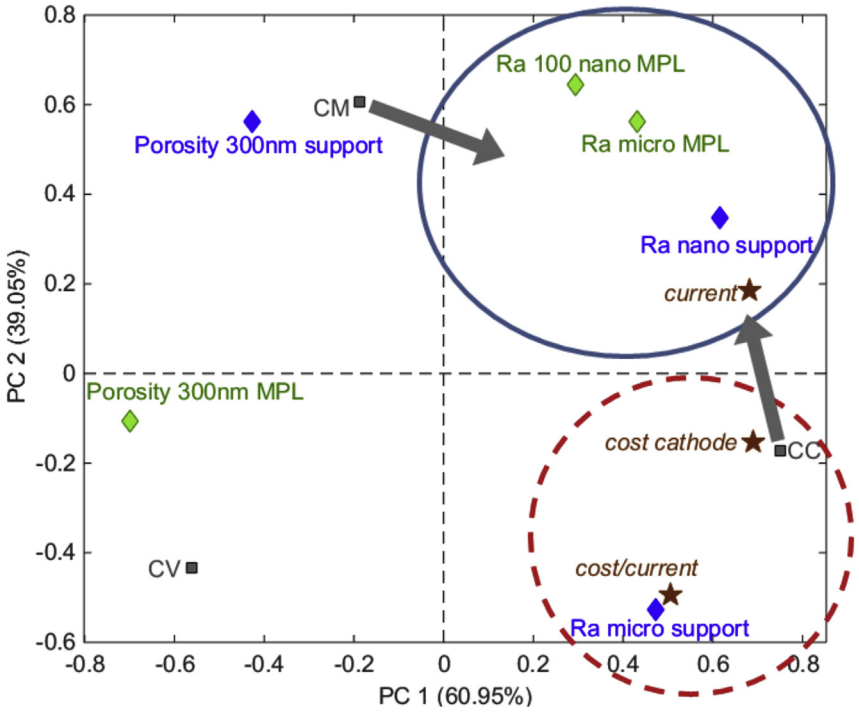

Fig. 8 – PCA bi-plot of current, cost, cost/current generated by the Fe-AAPyr and morphological properties of support and support with MPL. Squares are samples, diamonds and stars are variables.

Functionalizing the cathode surface is essential for the achievement of improved current generation. The optimal support has highest amount of oxygen containing functionalities present as reported by XPS. In general, Non-PGM Fe-AAPyr has shown to be a promising catalyst that could be applied on various low-cost, carbon-based substrates. Therefore, it is important to explore further its suitability for ceramic MFC applications in real operating conditions.

Despite those considerations, the current produced was generally low probably due to the scarce contact between the cathode and the ceramic. Further studies should be carried out in a direction of incorporating the catalytic layer directly onto the ceramic surface to minimize the ohmic resistance.

Conclusions

Carbon cloth (CC), carbon mesh (CM) and carbon veil (CV)) were studied as an electrode and current collector. CC performed better than CM and CV but CM was the most cost effective material. The addition of conductive paint (PA) and micro porous layer (MPL) boosted up the performances significantly with a two/three-fold increase. A linear relationship between roughness and skewness at the nanoscale and the current was found indicating that the modification probably enhanced the contact between the electrode and the ceramic separator. CM was the most cost effective materials with MPL addition. The addition of low cost platinum-free Fe-AAPyr as inorganic catalyst increased further the current generated.

Acknowledgment

This work has been financed by: i) the FSE-Lombardia, project "Luce bioelettrica" number 17157; ii) the Electrochemical Society and Billl & Melinda Gates Foundation under initiative: "Applying Electrochemistry to Complex Global Challenges" iii) Bill and Melinda Gates Foundation grant no. OPP1094890. Ioannis Ieropoulos is an EPSRC Career Acceleration Fellow supported by grant numbers EP/I004653/1 and EP/L002132/1.

REFERENCES

[1] Rinaldi A, Mecheri B, Garavaglia V, Licoccia S, Di Nardo P, Traversa E. Engineering materials and biology to boost performance of microbial fuel cells: a critical review. Energy Environ Sci 2008;1:417–29.
[2] Logan BE, Rabaey K. Conversion of wastes into bioelectricity and chemicals by using microbial electrochemical technologies. Science 2012;337(6095):686–90.
[3] Ieropoulos IA, Ledezma P, Stinchcombe A, Papaharalabos G, Melhuish C, Greenman J. Waste to real energy: the first MFC powered mobile phone. Phys Chem Chem Phys 2013;15(37):15312–6.
[4] Ieropoulos IA, Greenman J, Melhuish C, Horsfield I. Microbial fuel cells for robotics: energy autonomy through artificial symbiosis. Chem Sus Chem 2012;5(6):1020–6.
[5] Papaharalabos G, Greenman J, Melhuish C, Santoro C, Cristiani P, Li B, et al. Increased power output from micro porous layer (MPL) cathode microbial fuel cells (MFC). Int J Hydrogen Energy 2013;38(26):11552–8.

[6] Wei J, Liang P, Huang X. Recent progress in electrodes for microbial fuel cells. Biores Technol 2011;102:9335–44.
[7] Hamelers HVM, Ter Heijne A, Sleutels THJA, Jeremiasse AW, Strik DPBTB, Buisman CJN. New applications and performance of bioelectrochemical systems. Appl Microbiol Biotechnol 2010;85(6):1673–85.
[8] Franks AE, Nevin KP. Microbial fuel cells, a current review. Energies 2010;3:899–919.
[9] Rismani-Yazdi H, Carver SM, Christy AD, Tuovinen OH. Cathodic limitations in microbial fuel cells: an overview. J Power Sources 2008;180(2):683–94.
[10] Santoro C, Guilizzoni M, Correa Baena JP, Pasaogullari U, Casalegno A, Li B, et al. The effect of carbon surface properties on bacteria attachment and start up time of microbial fuel cells. Carbon 2014;67:128–39.
[11] Rabaey K, Rodrıguez J, Blackall LL, Keller J, Gross P, Batstone D, et al. Microbial ecology meets electrochemistry: electricity-driven and driving communities. ISME J 2007;1:9–18.
[12] Ishii S, Suzuki S, Norden-Krichmar TM, Phan T, Wanger G, Nealson KH, et al. Microbial population and functional dynamics associated with surface potential and carbon metabolism. ISME J 2014;8(5):963–78.
[13] Ishii S, Suzuki S, Norden-Krichmar TM, Wu A, Yamanaka Y, Nealson KH, et al. Identifying the microbial communities and operational conditions for optimized wastewater treatment in microbial fuel cells. Water Res 2013;47(19):7120–30.
[14] Xafenias N, Mapelli V. Performance and bacterial enrichment of bioelectrochemical systems during methane and acetate production. Int J Hydrogen Energy 2014;39(36):21864–75.
[15] Erable B, Feron D, Bergel A. Microbial catalysis of the oxygen reduction reaction for microbial fuel cells: a review. Chem Sus Chem 2012;5:975–87.
[16] Santoro C, Babanova S, Atanassov P, Li B, Ieropoulos I, Cristiani P. High power generation by a membraneless single chamber microbial fuel cell (SCMFC) using enzymatic Bilirubin oxidase (BOx) air-breathing cathode. J Electrochem Soc 2013;160(10):H720–6.
[17] Minteer SD, Liaw BY, Cooney MJ. Enzyme-based biofuel cells. Curr Opin Biotechnol 2007;18(3):228–34.
[18] Liew KB, Daud WRW, Ghasemi M, Leong JX, Lim SS, Ismail M. Non-Pt catalyst as oxygen reduction reaction in microbial fuel cells: a review. Int J Hydrogen Energy 2014;39:4870–83.
[19] Antolini E. Composite materials for polymer electrolyte membrane microbial fuel cells. Biosens Bioelectron 2015;69:54–70.
[20] Wang Z, Cao C, Zheng Y, Chen S, Zhao F. Abiotic oxygen reduction reaction catalysts used in microbial fuel cells. Chem Electro Chem 2014;1:1813–21.
[21] Cheng S, Liu H, Logan BE. Increased performance of single-chamber microbial fuel cells using an improved cathode structure. Electrochem Comm 2006;8:489–94.
[22] Feng Y, Shi X, Wang X, Lee H, Liu J, Qu Y, et al. Effects of sulfide on microbial fuel cells with platinum and nitrogen-doped carbon powder cathodes. Biosens Bioelectron 2012;35:413–5.
[23] Santoro C, Serov A, Narvaez Villarrubia CW, Stariha S, Babanova S, Schuler AJ, et al. Double chamber MFC with non-PGM Fe-N-c cathode catalyst. Chem Sus Chem 2015;8(5):828–34.
[24] Li B, Zhou X, Wang X, Liu B, Li B. Hybrid binuclear-cobalt-phthalocyanine as oxygen reduction reaction catalyst in single chamber microbial fuel cells. J Power Sources 2014;272:320–7.
[25] Liu B, Brückner C, Lei Y, Cheng Y, Santoro C, Li B. Cobalt porphyrin-based material as methanol tolerant cathode in single chamber microbial fuel cells (SCMFCs). J Power Sources 2014;257:246–53.
[26] Li X, Hu B, Suib S, Lei Y, Li B. Electricity generation in continuous flow microbial fuel cells (MFCs) with manganese dioxide (MnO_2) cathodes. Biochem Eng J 2011;54(1):10–5.
[27] Ledezma P, Stinchcombe A, Greenman J, Ieropoulos I. The first self-sustainable microbial fuel cell stack. Phys Chem Chem Phys 2013;15(7):2278–81.
[28] Ieropoulos IA, Greenman J, Melhuish C. Miniature microbial fuel cells and stacks for urine utilization. Int J Hydrogen Energy 2013;38(1):492–6.
[29] Karra U, Manickam SS, McCutcheon JR, Patel N, Li B. Power generation and organics removal from wastewater using activated carbon nanofiber (ACNF) microbial fuel cells (MFCs). Int J Hydrogen Energy 2013;38(3):1588–97.
[30] Zhang Y, Sun J, Hu Y, Li S, Xu Q. Bio-cathode materials evaluation in microbial fuel cells: a comparison of graphite felt, carbon paper and stainless steel mesh materials. Int J Hydrogen Energy 2012;37(22):16935–42.
[31] Erable B, Lacroix R, Etcheverry L, Féron D, Delia ML, Bergel A. Marine floating microbial fuel cell involving aerobic biofilm on stainless steel cathodes. Bioresour Technol 2013;142:510–6.
[32] Cristiani P, Carvalho ML, Guerrini E, Daghio M, Santoro C, Li B. Cathodic and anodic biofilms in single chamber microbial fuel cells. Bioelectro Chem 2013;92:6–13.
[33] Jang JK, Kan J, Bretschger O, Gorby YA, Hsu L, Kim B, et al. Electricity generation by microbial fuel cell using microorganisms as catalyst in cathode. J Microbiol Biotechnol 2013;23(12):1765–73.
[34] Babauta JT, Nguyen HD, Istanbullu O, Beyenal H. Microscale gradients of oxygen, hydrogen peroxide, and pH in freshwater cathodic biofilms. Chem Sus Chem 2013;6(7):1252–61.
[35] Popat SC, Ki D, Rittmann BE, Torres CI. Importance of OH^- transport from cathodes in microbial fuel cells. Chem Sus Chem 2012;5:1071–9.
[36] Santoro C, Cremins M, Pasaogullari U, Guilizzoni M, Casalegno A, Mackay A, et al. Evaluation of water transport and oxygen presence in single chamber microbial fuel cells with carbon-based cathodes. J Electrochem Soc 2013;160(7):G128–34.
[37] Kim JP, Cheng S, Oh S-E, Logan BE. Power generation using different cation, anion, and ultrafiltration membranes in microbial fuel cells. Environ Sci Technol 2007;41(3):1004–9.
[38] Zuo Y, Cheng S, Logan BE. Ion exchange membrane cathodes for scalable microbial fuel cells. Environ Sci Technol 2008;42(18):6967–72.
[39] Winfield J, Chambers LD, Rossiter J, Ieropoulos I. Comparing the short and long term stability of biodegradable, ceramic and cation exchange membranes in microbial fuel cells. Biores Technol 2013;48:480–6.
[40] Winfield J, Greenman J, Huson Ieropoulos I. Comparing terracotta and earthenware for multiple functionalities in microbial fuel cells. Bioprocess Biosyst Eng 2013;36(12):1913–21.
[41] Santoro C, Ieropoulos I, Greenman J, Cristiani P, Vadas T, Mackay A, et al. Power generation and contaminant removal in single chamber microbial fuel cells (SCMFCs) treating human urine. Int J Hydrogen Energy 2013;38:11543–51.
[42] Santoro C, Artyushkova K, Babanova S, Atanassov P, Ieropoulos I, Grattieri M, et al. Parameters characterization and optmization of activated carbon (AC) cathodes for microbial fuel cell applications. Biores Technol 2014;163:54–63.

[43] Li B, Zhou J, Zhou X, Wang X, Li B, Santoro C, et al. Surface modification of microbial fuel cell anodes: approaches to practical design. Electrochim Acta 2014;134:116–26.
[44] Brocato S, Serov A, Atanassov P. pH dependence of catalytic activity for ORR of the non-PGM catalyst derived from heat-treated Fe–phenanthroline. Electrochim Acta 2013;87:361–5.
[45] Gajda I, Greenman J, Melhuish C, Santoro C, Li B, Cristiani P, et al. Water formation at the cathode and sodium recovery using microbial fuel cells (MFCs). Sustain Energ Technol Assess 2014;7:187–94.